American Mineralogist, Volume 82, pages 979–990, 1997

Viscosity, fragility, and configurational entropy of melts along the join SiO_2-$NaAlSiO_4$

Michael J. Toplis,* Donald B. Dingwell, Kai-Uwe Hess, and Tommaso Lenci

Bayerisches Geoinstitut, Universität Bayreuth, D-95440 Bayreuth, Germany

Abstract

Viscosities of fourteen melts close to the join SiO_2-$NaAlO_2$ were measured in the range $1–10^{12}$ Pa·s (700–1650 °C) using a combination of concentric cylinder and micropenetration techniques. These compositions cover five isopleths in silica content from 50 to 82 mol% and vary from mildly peralkaline to mildly peraluminous. Greatly improved constraints on the temperature dependence of viscosity in the system SiO_2-$NaAlO_2$ result because exactly the same compositions were used for both high- and low-temperature measurements, viscosities over an extended range of silica contents were measured at temperatures close the glass transition, and several compositions at constant silica content and variable alkali/Al ratio were measured, allowing interpolation of data to compositions exactly along the join SiO_2-$NaAlO_2$. At high temperature (1600 °C) viscosity and activation energy are shown to be approximately a linear function of silica content, but large nonlinearities occur at temperatures close to the glass transition range. Defining fragility as the gradient of the viscosity curve at the glass transition temperature (T_g taken to be the 10^{12} Pa·s isokom) on a reduced temperature scale (T_g/T), it is found that the fragility increases in a nonlinear fashion as $NaAlO_2$ is substituted for SiO_2, with fragility increasing more rapidly at lower SiO_2 contents. The viscosity data are combined with heat capacity data available in the literature to estimate configurational entropies of albite, jadeite, and nepheline glasses using the Adam-Gibbs theory. Fragility, when defined in terms of the Adam-Gibbs parameters, is shown to increase with configurational heat capacity (difference in heat capacity between the liquid and the glassy states) but to decrease with increasing configurational entropy at the glass transition. In the light of independent phase equilibria and spectroscopic and calorimetric evidence that suggests the Al-Si ordering increases as silica content decreases from SiO_2 to nepheline, the modeling of configurational entropy in terms of Al-Si mixing suggests the following: (1) Melt configurational entropy has contributions from both cation mixing (chemical contribution), as well as variations in the topology of the O network (topological contribution), of which the latter dominates. (2) The chemical contribution is due to mixing of tetrahedral rather than O sites. (3) At the glass transition (10^{12} Pa·s isokom) the topological contribution shows little, if any, variation.

Introduction

Viscosity is a key parameter controlling the transport of silicate melts during a range of diverse processes relevant to glassmaking, nuclear and non-nuclear waste immobilization, igneous petrology, and volcanology. Although many viscosity measurements exist in the geological and glass-making literature (e.g., references in Bottinga and Weill 1972; Shaw 1972; Bansal and Doremus 1986; Mazurin et al. 1987, 1993), no robust predictive model of the compositional and temperature dependence of viscosity is presently available, particularly for temperatures close to the glass transition. It is, however, widely recognized that melt viscosity and structure are intimately related, and the most promising approaches to the prediction of structural relaxation time attempt quantitatively to relate this property to melt structure [e.g., mode-coupling theory (Götze 1991), free volume theory (Cohen and Grest 1979), and configurational entropy theory (Adam and Gibbs 1965)]. Of these three approaches the Adam-Gibbs theory has been shown to work remarkably well for a wide range of silicate melts (Richet 1984; Hummel and Arndt 1985; Tauber and Arndt 1987; Bottinga et al. 1995), being able quantitatively to account for non-Arrhenian behavior (i.e., deviation from the log viscosity being inversely proportional to absolute temperature), which is now recognized to be a characteristic of almost all silicate melts. Although the Adam-Gibbs theory has had much success in explaining many diverse features of the viscosities of silicate melts (e.g., Bottinga and Richet 1996), nevertheless, many details relating structure and configurational entropy remain unknown,

* Present address: CRPG-CNRS, BP20, F-54501, Vandoeuvre-lès-Nancy, France.

0003–004X/97/0910–0979$05.00

TABLE 1. ICP-AES analyses of studied samples

		NAS82: 52	NAS82: 50	NAS82: 48	NAS75: 53	NAS75: 50	NAS75: 47	NAS67: 55	NAS67: 50	NAS67: 47	NAS60: 52	NAS60: 50	NAS60: 48	NAS50: 51	NAS50: 49
Wt%	SiO_2	76.6	76.5	76.1	69.4	68.8	67.7	60.9	59.8	60.5	50.9	50.9	50.9	42.0	41.7
	Al_2O_3	14.0	14.3	14.9	17.9	19.2	20.7	22.4	25.3	26.0	28.2	29.2	30.5	35.1	36.5
	Na_2O	9.4	8.7	8.3	12.3	11.6	11.1	16.5	14.9	14.0	19.2	17.9	17.0	22.3	21.2
	Total	100.0	99.5	99.3	99.6	99.6	99.5	99.8	100.0	100.5	98.3	98.0	98.4	99.4	99.4
mol Na/(Na + Al)		52.5	50.0	47.8	53.1	49.8	46.9	54.8	49.2	47.0	52.8	50.2	47.8	51.1	48.9

and for the moment the Adam-Gibbs theory cannot be used in a predictive sense for compositionally complex silicate liquids. To further our understanding of the relationships between melt structure, entropy, and viscosity, we have chosen to study the system SiO_2-$NaAlO_2$. This system has been extensively studied spectroscopically (Taylor and Brown 1979; Seifert et al. 1982; McMillan et al. 1982; Murdoch et al. 1985; Matson et al. 1986; Neuville and Mysen 1996), and calorimetrically (Navrotsky et al. 1982; Richet and Bottinga 1984; Richet et al. 1990), as well as modeled at very high temperatures using molecular dynamics simulations (Scamehorn and Angell 1991; Stein and Spera 1995). Viscosity measurements also are numerous in this system (e.g., Riebling 1966; Taylor and Rindone 1970; Hunold and Brückner 1980; Cranmer and Uhlmann 1981; Stein and Spera 1993), but there is considerable disagreement between certain studies. Key questions remain unanswered such as how viscosity, activation energy, and departure from Arrhenian behavior all vary as a function of silica content along this join. This situation is largely due to (1) A lack of low temperature data for compositions poor in silica and (2) The fact that high- and low-temperature viscosities are often measured by different workers on different compositions. This may be particularly important because it is known that for melts close to the metaluminous join, small differences in the alkali/Al ratio may have a significant effect on viscosity (e.g., Richet and Bottinga 1984).

To provide the best possible constraints on viscosity along the join SiO_2-$NaAlO_2$ shear viscosities of melts containing between 50 and 82 mol% SiO_2 were measured over a wide range from 10^1 Pa·s to 10^{12} Pa·s. Several compositions of variable Na/Al ratio were studied at each silica isopleth to quantify the effect of small changes in alkali/Al ratio on viscosity. These data were then combined with calorimetric data from the literature and interpreted within the framework of the Adam-Gibbs theory to shed more light on the relationship between melt configurational entropy and structure.

EXPERIMENTAL METHODS

Starting compositions and sample preparation

Fourteen compositions along five isopleths in silica content in the system $NaAlO_2$-SiO_2 were studied with silica contents ranging from 82 to 50 mol% (Fig. 1). A series of glasses along silica isopleths were prepared by

TABLE 2. Viscosity determinations

NAS82	$\log_{10}\eta$ (Pas)			NAS75	$\log_{10}\eta$ (Pas)			NAS67	$\log_{10}\eta$ (Pas)		
T (°C)	82:52	82:50	82:48	T (°C)	75:53	75:50	75:47	T (°C)	67:55	67:50	67:47
1645			3.129	1621		2.716	2.726	1652			2.000
1621	2.929			1596	2.638	2.855	2.870	1643		1.969	
1596	3.053	3.331	3.417	1547	2.875	3.152	3.175	1594	1.900	2.227	2.321
1547	3.304	3.643	3.750	1497	3.119	3.465	3.504	1544	2.120	2.506	2.616
1497	3.579	3.967	4.105	1448	3.377	3.810	3.862	1495	2.343	2.799	2.925
1448	3.864	4.322	4.471	1399	3.663	4.182	4.250	1446	2.582	3.113	3.265
1399	4.171	4.704	4.871	1349	3.957	4.569	4.670	1396	2.828	3.446	
1349	4.485			1300	4.277			1347	3.089		
1300	4.827			1250	4.622			1298	3.366		
977.9			9.92	931.3			9.76	906.2			9.92
947.2			10.44	914.5			10.14	890.3			10.23
929.1			10.70	907.0		9.81		869.2			10.69
918.1		9.65		893.1			10.48	860.4		9.89	
912.8			11.15	893.0		10.05		854.0			11.33
880.4		10.38		875.2		10.38		842.2		10.25	
867.0	8.93			872.2			10.78	820.6		10.64	
846.8		11.04		867.3		10.58		802.4		11.24	
836.4	9.28			852.1	8.89			746.7	9.33		
810.5	9.73			848.9		10.95		728.4	9.79		
791.4	9.98			848.8			11.36	710.1	10.21		
755.8	10.67			823.8	9.22						
				812.1	9.46						
				794.1	9.79						
				772.7	10.30						
				748.2	10.78						

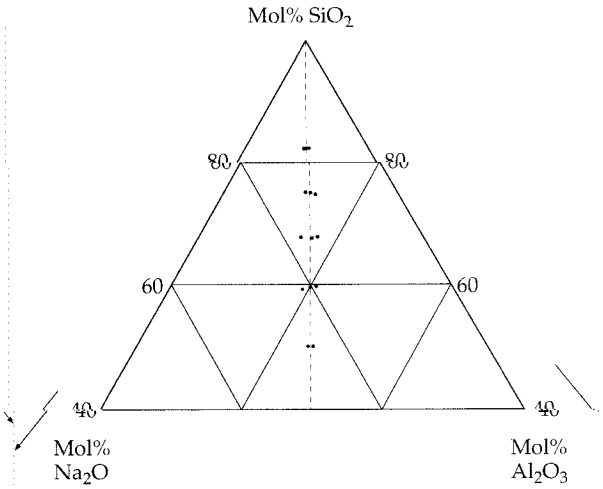

FIGURE 1. Compositions of the studied melts in an expanded portion of the system Na_2O-Al_2O_3-SiO_2.

fusing large batches (up to 200g) of peralkaline and peraluminous end-members (from mixtures of reagent grade SiO_2, Al_2O_3, and Na_2CO_3) in a 75 cm^3 thin-walled platinum crucible. These mixtures were held for one hour above their liquidus, in a molybdenum disilicide box furnace. Each of the end-members was then ground to a fine powder in a Retsch automatic agate mortar, and intermediate compositions were made from appropriate mixtures of the end-member glass powders.

Compositions were determined by ICP-AES from chips of glass recovered after homogenization during high-temperature viscosity measurements. A summary of the ICP-AES analyses is given in Table 1.

TABLE 2. *Continued*

NAS60	$\log_{10}\eta$ (Pas)			NAS50	$\log_{10}\eta$ (Pas)	
T (°C)	60:52	60:50	60:48	*T* (°C)	50:51	50:49
				1646	1.117	1.118
1643		1.627	1.641	1621	1.226	1.229
1623	1.657			1596	1.341	1.345
1594	1.801	1.871	1.889	1572	1.456	1.460
1544	2.047	2.136	2.161	1547	1.579	1.586
1495	2.298	2.418	2.452	891.3		9.46
1446	2.575	2.725	2.767	889.8	8.99	
1397	2.876	3.052	3.114	874.3		9.98
1348	3.199			865.1	9.57	
928.4			8.91	851.9		10.72
889.5			9.80	847.3	10.05	
876.9		9.35		844.8		10.78
856.2		9.75		829.4	10.73	
852.0			10.65	827.8		11.40
851.7	8.64					
843.6		10.00				
821.4		10.48				
813.7	9.44					
801.9		11.09				
774.7	10.36					
752.0	11.12					

Viscosity determinations

Shear viscosities in the range 1 to 10^5 Pa·s were measured at one atmosphere in air using the concentric cylinder method. This apparatus, and description of the platinum rhodium spindle and crucible geometries are described in Dingwell (1989) and Dingwell and Virgo (1987), respectively. A Brookfield DV-III viscometer head with a full scale torque of 7.20×10^{-2} N·m was used at rotation rates between 0.1 and 20 rpm, higher viscosities being measured at lower strain rates. Measurements were started at high temperature and the melt stirred until a stable viscosity reading was maintained for one hour. Subsequent measurements were carried out, lowering the temperature until either crystallization or an instrumental limit was reached. After the lowest temperature measurement, the highest temperature condition was reoccupied, and the comparison of first and last high-temperature measurements serves as a check against instrumental and compositional drift. Absolute viscosities were calculated by calibrating the crucible, spindle, and head combination using the National Institute of Standards and Testing lead-silicate glass SRM 711, and Deutsche Glastechnische Gesellschaft soda-lime glass DGG-1. The accuracy of the concentric cylinder method may be taken as ±5% (Dingwell 1989), but it should be noted that the precision of this technique is considerably better (less than ±0.5%, Toplis and Dingwell 1996).

Viscosities in the range 10^9 to 10^{12} Pa·s have been measured using a micropenetration technique on samples recovered from high temperature viscosity measurements. This method involves determining the rate at which a hemispherical iridium indenter (2 mm in diameter) moves into the melt surface under a fixed load of 1.2 N. These measurements were performed using a BÄHR DIL 802V vertical push-rod dilatometer, equipped with a silica sample holder under an argon-gas flow. Viscosities determined on lead-silicate SRM-711 have been reproduced within an error of ±0.06 log units. Further details of this apparatus may be found in Hess et al. (1995).

RESULTS

Measured viscosities are summarized in Table 2, and those for the 75, 67, and 50 mol% SiO_2 isopleths are shown graphically in Figure 2. For all of the studied melts it is clear that the Arrhenius relation (Eq. 1), which describes log viscosity ($\log_{10}\eta$) as a linear function of inverse absolute temperature (T) through two constants A_{Arr} and B_{Arr} is insufficient to describe the temperature dependence of viscosity of these melts over the studied temperature range.

$$\log_{10}\eta = A_{Arr} + \frac{B_{Arr}}{T} \quad (1)$$

An adequate description of the temperature dependence of viscosity is given by the three-parameter Tamann-Vogel-Fulcher Equation 2, with which the data shown in Figure 2 have been fitted and for which the constants

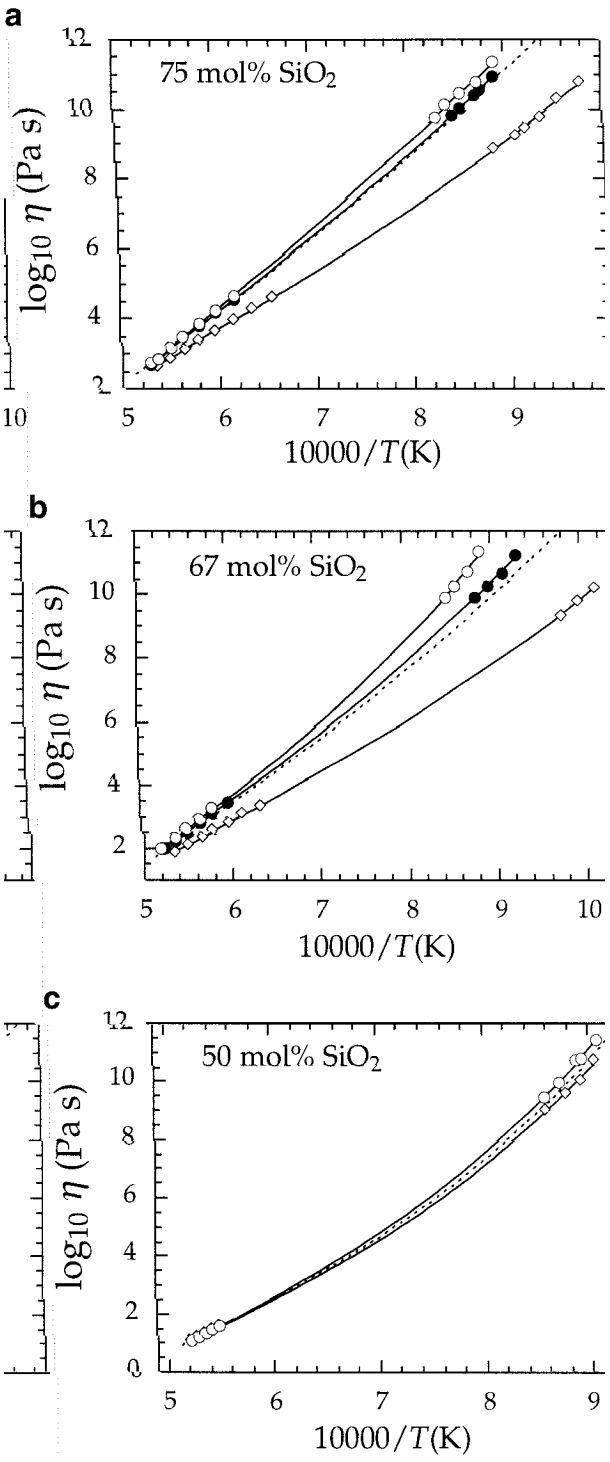

FIGURE 2. Viscosity data as a function of inverse temperature for (**a**) 75 mol% SiO_2, (**b**) 67mol% SiO_2, and (**c**) 50 mol% SiO_2. Open diamonds represent a mildly peralkaline composition (Na/Al > 1), filled circles represent a nominally metaluminous composition (Na/Al = 1), and open circles represent a mildly peraluminous composition (Na/Al < 1). Solid lines represent TVF fits to the viscosity data (see text and Table 3 for details). Dashed lines represent interpolated viscosity curves of compositions exactly along the join SiO_2-$NaAlO_2$.

TABLE 3. Parameters of TVF fits to measured viscosities

	A_{TVF}	B_{TVF}	C_{TVF}
NAS 82:52	−5.863(0.520)*	16446(1425)	28.9(57)
NAS 82:50	−5.783(0.630)	15170(3376)	214.7(130)
NAS 82:48	−6.760(0.630)	16208(1548)	278.0(55)
NAS 75:53	−4.074(0.334)	10498(713)	312.4(33)
NAS 75:50	−6.492(0.288)	15108(694)	254.3(26)
NAS 75:47	−7.460(0.520)	17108(1304)	211.7(45)
NAS 67:55	−3.953(0.309)	8911(622)	352.4(32)
NAS 67:50	−5.625(0.522)	11694(1113)	378.9(46)
NAS 67:47	−4.662(0.795)	9267(1492)	543.0(66)
NAS 60:52	−4.086(0.353)	8213(651)	481.5(32)
NAS 60:50	−5.611(0.312)	10757(646)	428.9(27)
NAS 60:48	−5.500(0.208)	10070(402)	502.7(17)
NAS 50:51	−4.283(0.303)	6910(514)	640.6(26)
NAS 50:49	−4.889(0.194)	7763(336)	623.9(16)

* Number in parentheses represents absolute error on the quoted value.

A_{TVF}, B_{TVF}, and C_{TVF} for each composition are shown in Table 3.

$$\log_{10}\eta = A_{TVF} + \frac{B_{TVF}}{T - C_{TVF}} \quad (2)$$

For all silica isopleths the mildly peralkaline compositions have much lower viscosities than those of melts closest to the join (Fig. 2). This is to be expected because peralkaline compositions contain non-bridging O atoms, whereas melts on the metaluminous join are generally considered to be fully polymerized. However, somewhat surprising is the fact that peraluminous melts consistently show higher viscosities than those of the composition closest to the metaluminous join (Fig. 2). The metaluminous join does not, therefore, represent a maximum in viscosity, and it is thus possible that such melts still contain a small proportion of non-bridging O atoms. This is discussed in some detail by Toplis et al. (1997), who concluded that the shift of the viscosity maximum into the peraluminous field can be explained by the presence of triclusters (Lacy 1963) consisting of a threefold-coordinated O atom, to which one aluminate and two silicate tetrahedra are attached.

Interpolated viscosities along the join SiO_2-$NaAlO_2$

The fact that viscosities were measured at constant silica content, but variable Na/(Na + Al) ratio permits interpolation of the data to obtain viscosities of melts exactly on the metaluminous join. These interpolated viscosities are compared with the measurements in Figure 2 (shown as a dashed line), and those of each of the five studied silica contents are compared in Figure 3, where important differences in both viscosity and departure from Arrhenian behavior are apparent. These differences are considered in more detail below. The viscosities of interpolated compositions exactly on the join SiO_2-$NaAlO_2$ have been fitted using Equation 2, as shown in Table 4. When the data from this study are combined with values for SiO_2 taken from Richet (1984) it is found that both B_{TVF} and C_{TVF} vary as an approximately linear function of silica content over the entire range 50–100 mol%.

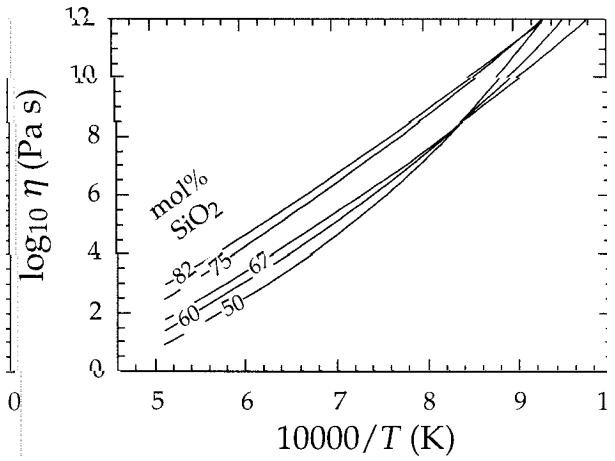

FIGURE 3. Interpolated viscosites of compositions exactly along the join SiO_2-$NaAlO_2$.

Comparison with previous studies

Several previous studies have looked at the viscosities of melts along the join SiO_2-$NaAlO_2$, in particular those corresponding in composition to the minerals albite ($NaAlSi_3O_8$) and jadeite ($NaAlSi_2O_6$). Our interpolated viscosity curves for compositions exactly on the join SiO_2-$NaAlO_2$ are compared in Figure 4 with literature data for albite, jadeite, and nepheline ($NaAlSiO_4$). There is generally good agreement between our results and those of previous studies, although our interpolated viscosities at temperatures close to the glass transition are slightly lower than those measured by Taylor and Rindone (1970), for both albite and jadeite melts. In comparison with Figure 2 it is clear that such small differences may be caused by small changes in the Na/(Na + Al) ratio. Indeed it is worth noting that although we tried to make compositions exactly on the join SiO_2-$NaAlO_2$, the greater part were slightly peraluminous and thus of higher viscosity than our interpolated composition. The same may also be true of compositions studied by Taylor and Rindone (1970) and Hummel and Arndt (1985). A more serious discrepancy occurs between our data and those of Hunold and Brückner (1980) for jadeite melt at low temperature for which no simple explanation has been found. In contrast to the conclusion of Stein and Spera (1993) we find the high-temperature determinations

TABLE 4. TVF parameters of interpolated compositions on the join SiO_2-$NaAlO_2$

SiO_2 (mol%)	A_{TVF}	B_{TVF}	C_{TVF}
100*	−7.262	26984	0
82	−5.783	15170	214.7
75	−6.385	14900	257.5
67	−5.743	12065	340.5
60	−5.655	10835	429.0
50	−4.586	7337	632.3

* Values taken from Richet (1984).

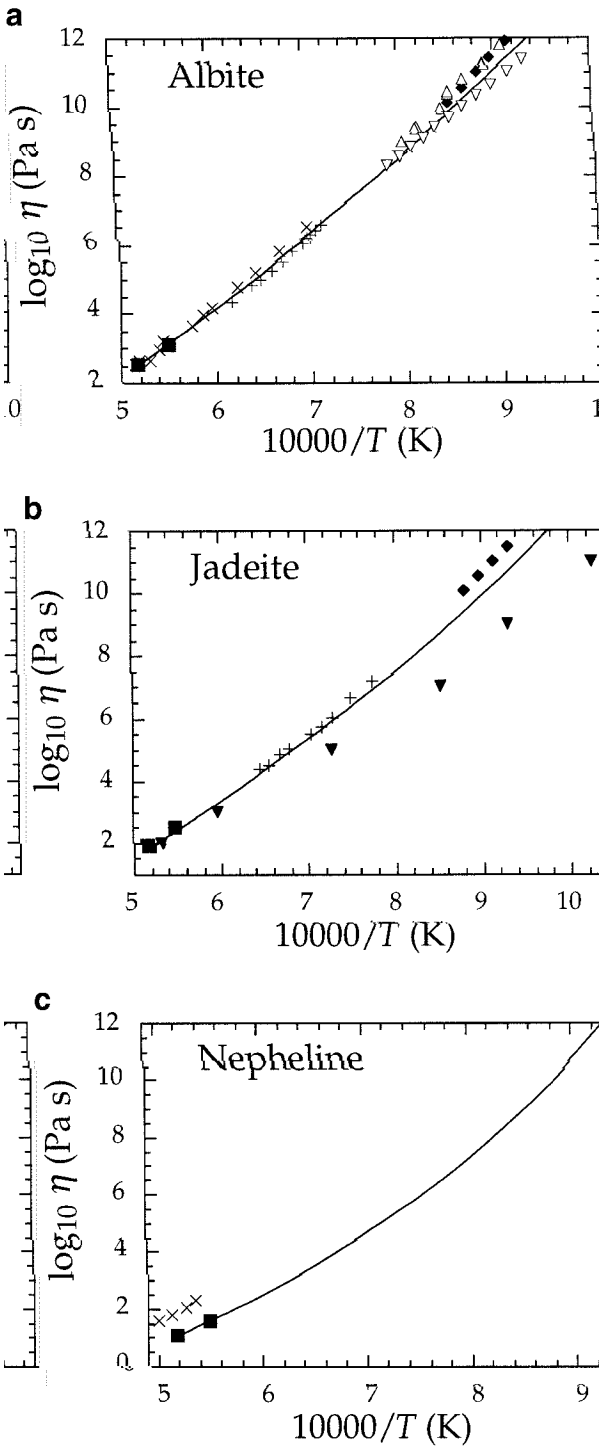

FIGURE 4. Comparison of interpolated viscosity curves (solid line) with literature values, for (**a**) albite, (**b**) jadeite, and (**c**) nepheline. Solid box = Riebling (1966); × = N'Dala et al. (1984); solid, inverted triangle = Hunold and Brückner (1980); + = Stein and Spera (1993); solid diamond = Taylor and Rindone (1970); open triangle = Hummel and Arndt (1985); open inverted triangle = Cranmer and Uhlmann (1981).

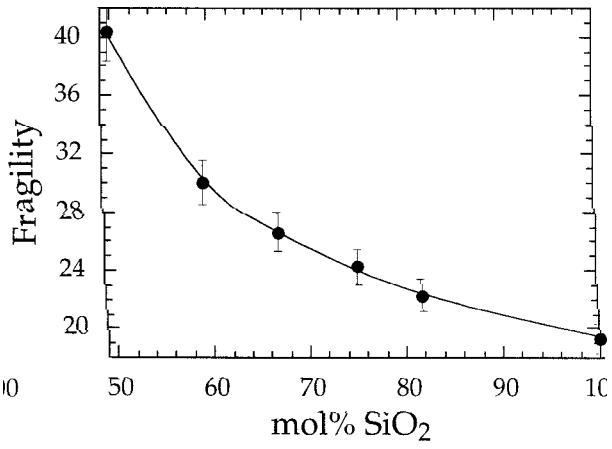

FIGURE 5. Variation of fragility as a function of silica content.

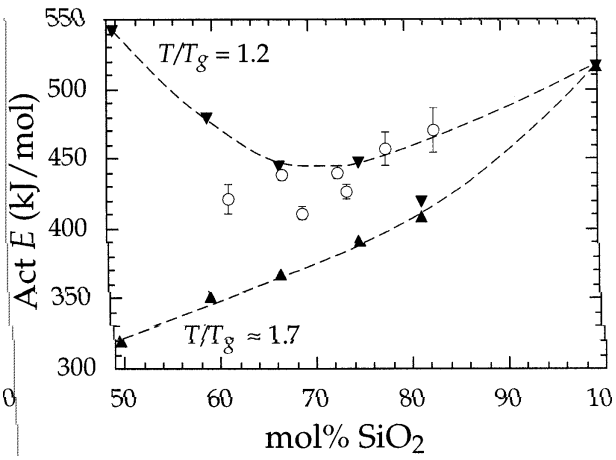

FIGURE 6. Variation of activation energy as a function of silica content. The solid triangle represents the slope of the log viscosity-inverse temperature relation calculated from measured viscosities (Table 2) in the range 1550–1600 °C ($T/T_g \approx 1.7$). The solid, inverted triangle represents the slope calculated from differentiation of the TVF equation (Table 4) at a temperature $T/T_g = 1.2$. Open circles are values reported by Stein and Spera (1993).

of Riebling (1966) to be in excellent agreement with the results presented here, not only for albite and jadeite melts, but also nepheline composition at high temperature, with the results of N'Dala et al. (1984) being one log unit too high in viscosity.

Albite and jadeite are the only compositions in this system for which a large enough viscosity range has been previously measured to constrain with any accuracy the TVF parameters. The value of C_{TVF} obtained for albite melt in this study (257.5 K) agrees well that of 277 K reported by Richet (1984) and 274 K reported by Stein and Spera (1993), while our value for jadeite melt (340.5 K) lies between the values of 297 K and 477 K reported by Stein and Spera (1993) and Richet (1984), respectively.

Departure from Arrhenian behavior and fragility

The departure of viscosity from an Arrhenian temperature dependence is commonly discussed using the concept of fragility (Angell 1985) where strong melts show behavior approaching that of the Arrhenian case, and weak, or fragile melts show large departures. Compared with many organic polymers and molecular liquids, silicate melts are in general strong, although as can be seen from Figures 2 and 3, important departures from Arrhenian behavior do occur. The definition of fragility as the gradient of the viscosity curve at the glass transition temperature on a reduced temperature scale (Plazek and Ngai 1991; Böhmer and Angell 1992) is commonly used and has been found to be one of the most satisfactory (Hess 1996). Fragility may therefore be calculated by differentiating the TVF equation:

$$\text{fragility} = m = \left.\frac{\mathrm{d}(\log_{10}\eta)}{\mathrm{d}(T_g/T)}\right|_{T=T_g} = \frac{B_{TVF}}{T_g(1 - C_{TVF}/T_g)^2} \quad (3)$$

Using Equation 3, we define T_g to be the 10^{12} Pa·s isokom [with laboratory cooling rates on the order of 10 K/s, the glass transition temperature defined calorimetrically has been shown to be close to the temperature at which the viscosity is 10^{12} Pa·s (see Richet and Bottinga 1995)]. Thus we find that the fragility of compositions along the studied join increases, but in a non-linear manner as a function of SiO_2 content with little or no increase in fragility between pure SiO_2 and 82 mol% SiO_2, but ever increasing fragility at lower silica contents (Fig. 5). These data therefore unambiguously confirm that fragility increases from SiO_2 to nepheline, as indicated by the data of Stein and Spera (1993). Such data are also in agreement with molecular dynamics simulations of these melts (Scamehorn and Angell 1991; Stein and Spera 1995).

Viscosity and activation energy on the join SiO_2-$NaAlO_2$

As shown by Figure 3, the increasingly fragile nature of melts, varying from pure SiO_2 to nepheline, results in the consequence that the concept of activation energy (the slope of the log viscosity–inverse temperature relation) should be used with extreme caution. For example, the slope of the log viscosity–inverse temperature relation for albite melt varies by 100 kJ/mol from the glass transition to 2000 K, while that of nepheline melt varies by over 600 kJ/mol. Despite such large variations in activation energy over the studied range of viscosity a meaningful comparison of activation energies may be made at fixed reduced temperature (T/T_g). Activation energies calculated from data in the range 1550 to 1600 °C ($T/T_g \approx 1.7$) show an almost linear decrease as a function of SiO_2 content, whereas at lower reduced temperature ($T/T_g = 1.2$) activation energy has a markedly non-linear dependence on silica content, with a minimum occurring close to 70 mol% SiO_2 (Fig. 6). At even lower reduced temperatures this minimum moves to higher silica contents. Stein and Spera (1993) performed viscosity measurements for sev-

en different silica contents over a 250 °C temperature range (approximately T/T_g = 1.2–1.35). In this range they fitted their data using the Arrhenian Equation 1 and presented a single value of activation energy for each of the studied compositions. As might be expected, at high silica contents their values approach those reported here for T/T_g =1.2, being consistently higher than those for T/T_g = 1.7. The scatter and lack of clear trend for activation energy reported by Stein and Spera (1993) at lower SiO_2 contents may therefore be explained in terms of the increasingly non-Arrhenian nature of these melts and increasing sensitivity of activation energy to temperature.

Viscosity shows a similar behavior, so that at high temperature log viscosity may be adequately described as a linear function of SiO_2 content (Fig. 7a). At lower temperatures, however, there is a clear departure from a linear dependence on silica content, with a minimum developing close to 67 mol% SiO_2 (Fig. 7b). This behavior is similar to that for melts along the join SiO_2-$CaAl_2O_4$, which show a minimum in T_g for compositions between 30 and 40 mol% SiO_2 (Neuville 1992).

Discussion

Adam-Gibbs theory and calculation of configurational entropies

The systematic variations in melt viscosity and fragility along the join SiO_2-$NaAlSiO_4$ described above, may be related to variations in configurational parameters of the melt using the Adam-Gibbs theory (Adam and Gibbs 1965; Richet 1984). This theory relates relaxation time of a melt (and thus its viscosity) to temperature and configurational entropy through the general equation:

$$\log_{10}\eta(T) = A_e + \frac{B_e}{TS_c(T)} \quad (4)$$

where η (T) is the viscosity, A_e and B_e are constant for each melt composition, and $S_c(T)$ is the configurational entropy of the melt at absolute temperature T. The Adam-Gibbs theory has been shown to account quantitatively for departures from Arrhenian behavior of a large range of silicate melts (e.g., Richet 1984; Richet and Neuville 1992; Bottinga et al. 1995; Bottinga and Richet 1996). Such departures occur because the configurational entropy of the melt is not a constant but is itself a function of temperature. At a given temperature the configurational entropy of the melt phase [$S_c(T)$] is the sum of that present at the glass transition $S_c(T_g)$, plus additional configurational entropy produced with increasing temperature. This additional entropy may be calculated by integration of the configurational heat capacity (C_p^{conf}), such that:

$$S_c(T) = S_c(T_g) + \int_{T_g}^{T} \frac{C_p^{conf}}{T}\,dT \quad (5)$$

where C_p^{conf} is given by $[C_p^{liq}(T) - C_p^{glass}(T_g)]$ that may itself be a function of temperature. The configurational heat capacities of albite, jadeite, and nepheline melts are known (reported in Fig. 8a), thus the viscosity curves

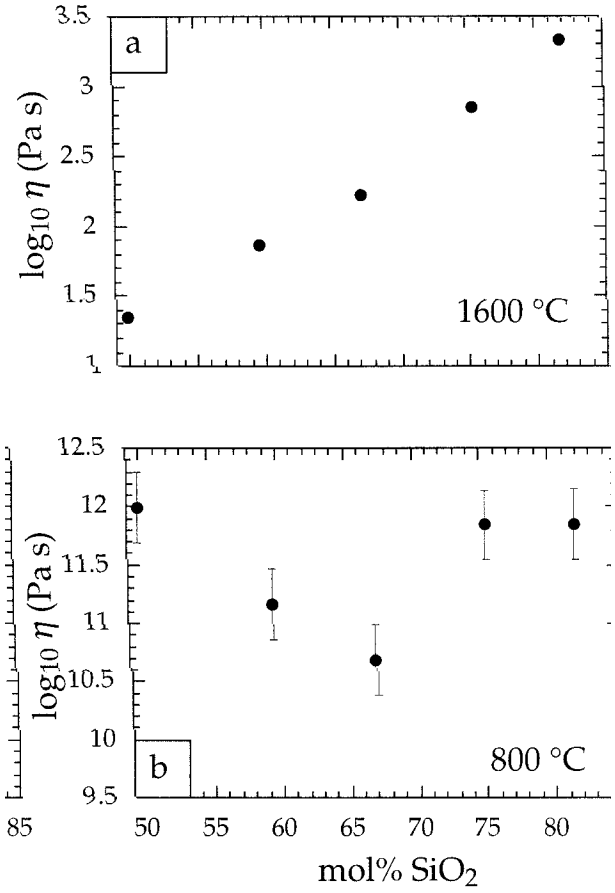

Figure 7. Variation of viscosity as a function of silica content at (**a**) 1600 °C ($T/T_g \approx 1.7$), and (**b**) 800 °C ($T/T_g \approx 1$).

may be fitted using A_e, B_e, and $S_c(T_g)$ as adjustable parameters (see Richet 1984; Bottinga and Richet 1996 for details).

The parameters obtained in the above manner are summarized in Table 5 and values for the configurational entropy at the glass transition are shown in Figure 8b. Combining these values with data for SiO_2 (Richet and Bottinga 1984), it is inferred that $S_c(T_g)$ increases from SiO_2 to albite, shows little change in the range 75 to 67 mol% SiO_2, but decreases significantly in the range 67 to 50 mol% SiO_2. These values of $S_c(T_g)$ obtained from the viscosity curves may be compared with independently measured values of this parameter using appropriate thermodynamic cycles of melt, glass, and crystalline phases (also shown in Fig. 8b). The agreement for albite melt is very good, but the value obtained in this study for nepheline melt [7.4 J/(gfw·K)] is considerably higher than that obtained from the calorimetric data of Richet et al. (1990) [4.9 J/(gfw·K)]. There are several reasons why this should be so. First, the values of $S_c(T_g)$ obtained from calorimetric cycles are calculated from a relatively small difference between two large numbers and are thus prone to large relative errors, in particular those associated with entropies of fusion or solid phase transitions. The second

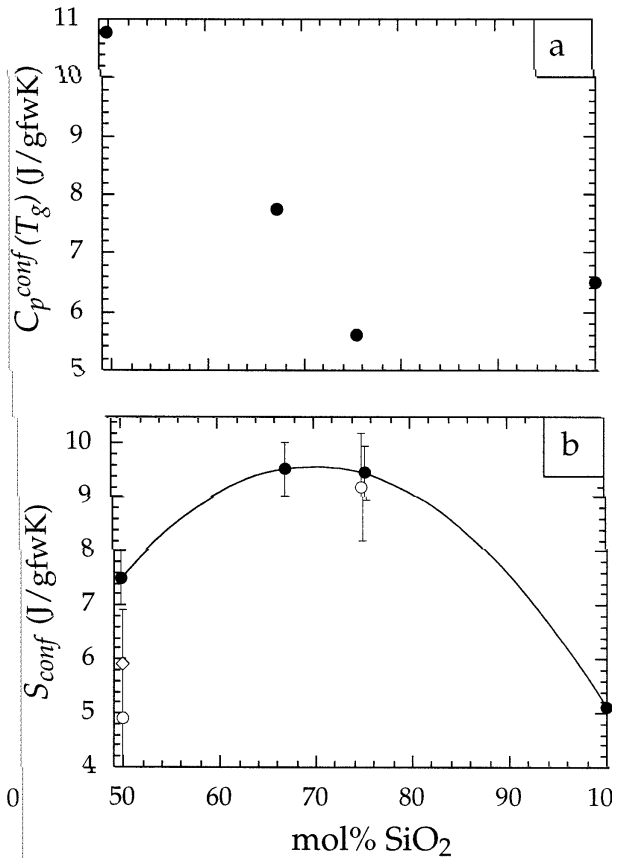

FIGURE 8. (**a**) Configurational heat capacity at the glass transition for compositions along the join SiO_2-$NaAlSiO_4$ (data from Richet 1984; Richet and Bottinga 1984; Richet et al. 1990). Note: gram formula weight (gfw) is defined such that molar (Na_2O + Al_2O_3 + SiO_2) = 1. (**b**) Configurational entropy at the glass transition calculated from the viscosity curve, using the Adam-Gibbs theory (solid circles). Also shown are values of $S_c(T_g$ determined calorimetrically (open circles, Richet 1984; Richet et al. 1990), as well as a corrected value for nepheline melt (open diamond), taking account of the different values used for T_g.

reason is that Richet et al. (1990) chose a value of 990 K for the glass transition temperature of nepheline composition, whereas the viscosity data suggest that the 10^{12} Pa·s isokom occurs at the significantly higher temperature of 1065 K. If the calorimetric data of Richet et al. (1990) are used to calculate the entropy of nepheline melt at 1065 K, a value of 5.9 ±1 J/(gfw·K) is obtained, thus within error much closer to the value obtained from the viscosity curve.

Melt fragility and the Adam-Gibbs theory

Many papers have dealt with application of the Adam-Gibbs theory to the explanation of departure from Arrhenian behavior, and, as noted by Adam and Gibbs themselves (Adam and Gibbs 1965), it is generally recognized that the greater the jump in C_p at the glass transition, the greater the fragility of the melt. However, it is clear that

TABLE 5. Heat capacities and parameters of the Adam-Gibbs equation

SiO_2 (mol%)	C_p^{conf} [J/(gfw·k)]* a†	10^3 b†	A_e	B_e	$S_{c(Tg)}$ [J/(gfw·k)]
75	−5.984	10.655	−2.45	145 800	9.45
67	−3.743	10.448	−2.52	141 000	9.52
50	−1.645	12.970	−2.38	116 100	7.51

* As discussed in the text, $C_p^{conf} = [C_p^{liq} - C_p^{glass}(T_g)]$, which for compositions along the join SiO_2-$NaAlSiO_4$ may be described by the equation $a + bT$, where a and b are constants, and T is absolute temperature.

† Values for the heat capacity of melt and glassy phases taken from Richet (1984), Richet and Bottinga (1984), and Richet et al. (1990). Note that gram formula weight (gfw) is defined such that molar (Na_2O + Al_2O_3 + SiO_2) = 1.

using the definition of fragility given by Equation 3, we may quantify fragility in terms of the Adam-Gibbs parameters. If the configurational heat capacity may be described as a linear function of temperature (i.e., $C_p^{conf} = a + bT$), which is the case for melts on the join SiO_2-$NaAlSiO_4$ (Richet and Bottinga 1984), then from Equations 4 and 5 it may be seen that in terms of the Adam-Gibbs parameters melt viscosity is:

$$\log_{10}\eta = A_e + \frac{B_e}{\{T[S_c(T_g) + a[\ln(T/T_g)] + b(T - T_g)]\}} \quad (6)$$

Differentiation of this equation with respect to T_g/T shows that at T_g, the gradient on a reduced temperature plot (and thus the fragility) is given by:

$$m = \frac{B_e}{S_c(T_g)T_g}\left[1 + \frac{a + bT_g}{S_c(T_g)}\right] \quad (7)$$

which may be simplified to:

$$m = \frac{B_e}{S_c(T_g)T_g}\left[1 + \frac{C_p^{conf}(T_g)}{S_c(T_g)}\right] \quad (8)$$

where $C_p^{conf}(T_g)$ is the jump in heat capacity at the glass transition. A simplification to Equation 8 occurs because if the glass transition is defined to occur when the viscosity reaches a value of 10^{12} Pa·s then from Equation 4:

$$\frac{B_e}{S_c(T_g)T_g} = 12 - A_e \quad (9)$$

Based on the observation that A_e is approximately constant, at least for the studied compositions (Table 5), then the term on the left hand side of Equation 9 is constant, therefore implying that fragility is proportional to:

$$1 + \frac{C_p^{conf}(T_g)}{S_c(T_g)} \quad (10)$$

Fragility (as defined by Eq. 3) is thus controlled not only by the magnitude of the configurational heat capacity at the glass transition but also by the configurational entropy of the melt at the glass transition temperature, with more fragile melts having a greater $C_p^{conf}(T_g)$, a lower $S_c(T_g)$, or both.

In the system SiO_2-$NaAlSiO_4$, data from the literature show $C_p^{conf}(T_g)$ is more or less constant in the range 100–75% SiO_2 (Fig. 8a), while the data from this study show that over the same range of silica content the configurational entropy at the glass transition increases (Fig. 8b) and the combination of these two factors correlates with little if any increase in fragility (Fig. 5). In the range 75–67 mol% SiO_2 the configurational entropy at the glass transition is approximately constant, but the configurational heat capacity is increasing, correlating with an increase in fragility. At lower silica contents, the configurational entropy at the glass transition decreases, and the configurational heat capacity increases, with both factors contributing to the rapid increase in fragility observed in this range of SiO_2 contents (Fig. 5). No predictions of the magnitude of the parameters B_{TVF} and C_{TVF}, or melt fragility may be made at silica contents less than 50 mol%, as the variation of $S_c(T_g)$ in this range is unknown.

It should be noted that the definition of fragility used here (Eq. 3), or indeed any single parameter definition of fragility, cannot fully parameterize non-Arrhenian behavior. For example there are families of TVF fits that have different B_{TVF} and C_{TVF} parameters, but the same gradient at the glass transition temperature. Similarly, although the gradient at T_g is defined by the configurational heat capacity at the glass transition temperature this does not take account of the temperature dependence of C_p^{conf}, which may be positive, zero or negative, behaviors shown by aluminosilicates, alkali-silicates, and titanosilicates, respectively (Richet and Bottinga 1995). Each of these cases results in a different temperature dependence of viscosity, even if the gradient at T_g is the same.

Configurational entropy at the glass transition

The aim of this section is to relate the calculated configurational entropies of glasses along the join SiO_2-$NaAlSiO_4$ to their structure. As discussed by Richet and Neuville (1992), there are two principal contributions to the configurational entropy of a silicate melt-glass. The first is due to mixing of chemically distinguishable units (the chemical contribution) and the second is due to distributions in bond angles and bond lengths (the topological contribution). Although the topological contribution is difficult to quantify, an attempt is made to model quantitatively the chemical contribution to the configurational entropy in terms of independent evidence concerning the structure of melts and glasses in this system.

Glasses along the join SiO_2-$NaAlSiO_4$ have been extensively studied spectroscopically (Taylor and Brown 1979; Seifert et al. 1982; McMillan et al. 1982; Murdoch et al. 1985; Matson et al. 1986; Oestrike et al. 1987; Maekawa et al. 1991; Neuville and Mysen 1996), and it is generally agreed that such compositions consist of a fully polymerized network of tetrahedral Si and Al, with Na stabilizing Al in this configuration. Furthermore, there is also evidence from a variety of sources concerning the state of Al-Si order-disorder in this system. For example, Flood and Knapp (1968) showed that although almost perfectly disordered, a small degree of Al-Si ordering was necessary to fit the liquidus surface of albite in the high silica range. In contrast, at silica contents near 50 mol% the calorimetric study of Navrotsky et al. (1982) showed that the greatest heat of mixing on the join SiO_2-$NaAlO_2$ occurred close to nepheline composition, implying a high degree of Si-Al order for this composition. An increase in Al-Si ordering with decreasing silica content was also suggested by Murdoch et al. (1985) who showed that the linewidth of ^{29}Si NMR spectra of nepheline glass was considerably less than that of albite glass, implying greater compliance with Loewensteins (1954) aluminium avoidance principle.

Within the framework of this structural model for glasses along the join SiO_2-$NaAlSiO_4$ the chemical contribution to configurational entropy is modeled by mixing of Al and Si. The first step is to define the mixing units. We have chosen to evaluate two possibilities: (1) O environments (e.g., Si-O-Si, Si-O-Al, etc.), and (2) tetrahedral environments (e.g., SiO_2, $NaAlO_2$). For each of these possibilities, entropies depend on the degree of Si-Al ordering, ranging from perfect disordering (where Al-O-Al, Si-O-Al, and Si-O-Si bonds may all occur) to ordering because of Al avoidance (Al-O-Al bonds forbidden, Loewenstein 1954), as shown in Figures 9a and 9b. In the case of mixing of tetrahedral or O atom sites the configurational entropy is zero for SiO_2, and initially increases as Al is substituted for Si. If Al-Si were to be perfectly disordered, then a smooth increase in S_c would occur going from silica to nepheline. In contrast, entropy in the perfectly ordered case would reach a maximum at albite composition before falling back to zero at nepheline composition. However, the absolute values of entropies calculated for the mixing of O or tetrahedral sites are very different. Entropies because of the mixing of O are much greater than those resulting from the mixing of tetrahedra, because of the greater number of the former per gram formula weight of melt. However, in neither of these two cases do the entropies estimated from the viscosity data lie between the ordered and the disordered case (Figs. 9a and 9b). This discrepancy may be expected because the modeled values presented in Figures 9a and 9b only represent the chemical contribution to S_c and do not take into account the topological contribution.

In the case of mixing of O sites it is clear that no positive value for the topological contribution can reconcile the modeled configurational entropies with those calculated from the viscosity curves. Thus it seems unlikely that the chemically distinct units in these melts are O atoms. On the other hand, values of configurational entropy modeled using tetrahedral sites are always lower than those calculated from the viscosity measurements, consistent with a topological contribution to the latter. If data for pure SiO_2 glass are used to estimate, to a first approximation, the magnitude of the topological contribution to glasses along the join SiO_2-$NaAlSiO_4$ (5.1 J/(gfw·K), Richet and Bottinga 1984), then it is found that the modeled values for the chemical contribution lie in

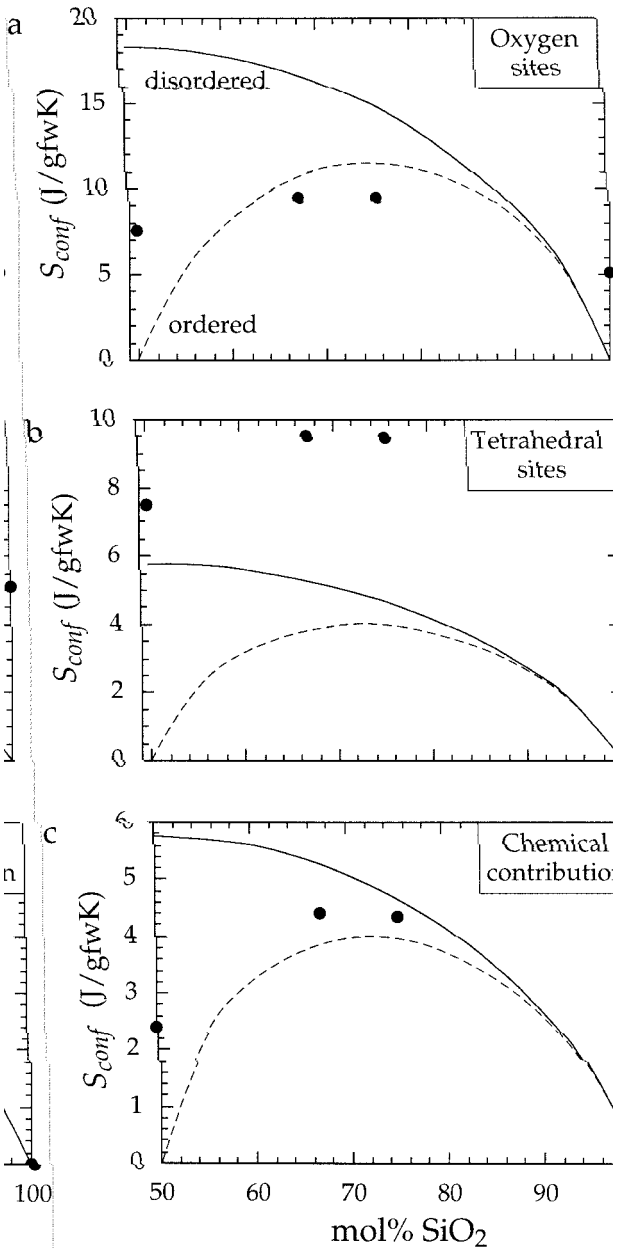

FIGURE 9. Configurational entropies modelled for perfect Al-Si ordering (dashed line) and perfect Al-Si disordering (solid line). Values estimated from the viscosity curves are shown as solid circles in the following cases: (**a**) if mixing is of different O sites; (**b**) if mixing is of different tetrahedral sites; and (**c**) modeled configurational entropies resulting from mixing of tetrahedral sites compared with estimates of the chemical contribution to the configurational entropy (= total configurational entropy − topological contribution). Total configurational entropy estimated from the viscosity data (Table 5). A constant topological contribution of 5.1 J/(gfw·K) was assumed (see text for details).

the range bracketed between values calculated for perfect ordering and perfect disordering of tetrahedral sites (Fig. 9c). Furthermore, it is found that albite glass occurs close to the limit for Al-Si disordering, while nepheline tends to the side of ordering, in agreement with the independent evidence described above. Although a constant value of $S_c(T_g)$ for all compositions is not required, it is clear that if the values of total configurational entropy are to remain within the bounds suggested by the modeling of the chemical contribution in terms of tetrahedral sites, as well as remaining consistent with the independent evidence that Al-Si ordering increases as silica content decreases from SiO_2 to nepheline, then the topological contribution to $S_c(T_g)$ along the studied join must be relatively constant [i.e., 6 ±1 J/(gfw·K)].

Configurational entropy at high temperature

With increasing temperature new topological and new chemical entropies may be produced, both contributing to C_p^{conf}. On one hand, molecular dynamics simulations of these melts show that at 3000 K there is a purely statistical random distribution of aluminate and silicate tetrahedra (Scamehorn and Angell 1991; Stein and Spera 1995). In contrast, the evidence summarized above suggests that at the glass transition there is considerable Al-Si ordering. Since the state of ordering both in the glass and at 3000 K are known, the contribution to the configurational heat capacity because of new chemical configurational entropy can be quantified. This calculation was previously performed by Scamehorn and Angell (1991) who concluded that randomization of Al-Si could be the dominant contribution to the configurational heat capacity for nepheline melt. However, Scamehorn and Angell (1991) assumed that mixing occurred on O sites, as well as assuming that nepheline melt was perfectly ordered when performing their calculations. Using the value for the chemical entropy of nepheline glass from this study and assuming that randomization of tetrahedral sites is complete by 3000 K, the contribution to C_p^{conf} will be approximately 3.5 J/(gfw·K), compared with the measured value of C_p^{conf} that varies between 12.7 J/(gfw·K) at T_g to 22.2 J/(gfw·K) at 1800 K (Richet et al. 1990). Contributions to C_p^{conf} from disordering of Al-Si are much smaller for albite and jadeite melts, and we therefore conclude that increases in topological entropy are the dominant contribution to C_p^{conf}. If this is true, then the increasing values of C_p^{conf} with decreasing silica content, as well as their increasing temperature dependence (Richet and Bottinga 1984, Richet et al. 1990), therefore implies that at high temperature the distribution of bond angles and lengths should increase as $NaAlO_2$ is substituted for SiO_2. Indeed, this is the prediction of molecular dynamics simulations of these melts at very high temperatures (Scamehorn and Angell 1991; Stein and Spera 1995).

Implications for generalized silicate melts

The results presented here have several implications for the structure-property relations of silicate melts in gen-

eral. First, our results, as well as those of Richet (1984) and Neuville and Richet (1991), show that variations in entropy across binary joins may be well modeled in terms of cation mixing. This is equivalent to considering the melt as a lattice of O atoms in which cations are distributed. The configurational entropy of the melt is the sum of that from the cation distribution within the O lattice (the chemical contribution) plus a background entropy because of variations in the topology of the O network (the topological contribution). Given that the O lattice represents the greater part of the volume of silicate melts, it does not seem unreasonable that topological contributions to the configurational entropy dominate. The fact that the topological contribution to the configurational entropy of the studied compositions is relatively constant at the glass transition may be linked to the fact that these glasses have very similar fully polymerized structures (and therefore O lattices). It would, however, be of interest to determine whether the glass transition of depolymerized silicate melts at laboratory cooling rates (e.g., 10 K/s) is also associated with a constant value of the topological contribution to the configurational entropy, in which case this may be the phenomenon responsible for the calorimetric glass transition.

Second, in agreement with findings in other silicate systems (Brandriss and Stebbins 1988; Richet and Neuville 1992), we find that increases in chemical entropy only represent a fraction of the configurational heat capacity, leaving increases in the topological contribution to dominate C_p^{conf}. In other words, as noted by Richet and Neuville (1992), it is above all the ability of O to explore new configurations, which increases the entropy and decreases the viscosity of silicate melts with increasing temperature. The ability of O to explore new configurations may be expected to be a function of the strength of its bonding with cations in the lattice, thus C_p^{conf} should be proportional to the average bond strength of the melt. Indeed at high temperature (e.g., 1800 K), C_p^{conf} for melts on the join SiO_2-$NaAlSiO_4$ as well as many other binary silicate joins is approximately a linear function of silica content (Richet and Bottinga 1985; Richet and Neuville 1992), supporting this hypothesis. Furthermore, because C_p^{conf} is the dominant factor affecting high-temperature viscosity (Eqs. 4 and 5), this too should also be directly proportional to average bond strength. Not only is this supported by the linear variation of viscosity as a function of silica content presented in this study (Fig. 7a), but perhaps the clearest evidence that this is true is the fact that Bottinga and Weill (1972) were successfully able to parameterize high-temperature viscosities as a linear function of composition. This study, which builds a better understanding of the relationships between melt structure and configurational entropy, is an important complementary step toward predicting silicate melt viscosities at temperatures close to the glass transition.

Acknowledgments

Anna Dietel is thanked for ICP-AES analyses of glasses. M.J.T. gratefully acknowledges financial support from the European Union, Human Capital and Mobility programme during the course of this work. Financial support for K.U.H. and T.L. was provided from Deutsche Forschungsgemeinschaft grant Di 431/3-2 to DBD. Daniel Neuville, Daniel Stein, and Rebecca Lange are thanked for their thorough and helpful reviews.

References cited

Adam, G. and Gibbs, J.H. (1965) On the temperature dependence of cooperative relaxation properties in glass-forming liquids. Journal of Chemical Physics, 43, 139–146.

Angell, C.A. (1985) Strong and fragile liquids. In K.L. Ngai and G.B. Wright, Eds., Relaxations in complex systems, p. 3–11. U.S. Department of Commerce National Technical Information Service, Springfield, Virginia.

Bansal, N.P. and Doremus, R.H. (1986) Handbook of glass properties. 680 p. Academic Press.

Böhmer, R. and Angell, C.A. (1992) Correlations of the nonexponentiality and state dependence of mechanical relaxations with bond connectivity in Ge-As-Se supercooled liquids. Physical Review B, 45, 10091–10094.

Bottinga, Y. and Richet, P. (1996) Silicate melt structural relaxation: rheology, kinetics, and Adam-Gibbs theory. Chemical Geology, 128, 129–141.

Bottinga, Y. and Weill, D.F. (1972) The viscosity of magmatic liquids: a model for calculation. American Journal of Science, 272, 438–475.

Bottinga, Y., Richet, P., and Sipp, A. (1995) Viscosity regimes of homogeneous silicate melts. American Mineralogist, 80, 305–318.

Brandriss, M.E. and Stebbins, J.F. (1988) Effects of temperature on the structures of silicate liquids: ^{29}Si NMR results. Geochimica et Cosmochimica Acta, 52, 2695–2669.

Cohen, M.H. and Grest, G.S. (1979) Liquid-glass transition, a free volume approach. Physical Review B, 20, 1077–1098.

Cranmer, D. and Uhlmann, D.R. (1981) Viscosity of liquid albite, a network material. Journal of Non-Crystalline Solids, 45, 283–288.

Dingwell, D.B. (1989) Shear viscosities of ferrosilicate liquids. American Mineralogist, 74, 1038–1044.

Dingwell, D.B. and Virgo, D. (1987) The effect of oxidation state on the viscosity of melts in the system Na_2O-FeO-Fe_2O_3-SiO_2. Geochimica et Cosmochimica Acta, 51 195–205.

Flood, H. and Knapp, W.J. (1968) Structural characteristics of liquid mixtures of feldspar and silica. Journal of the American Ceramic Society, 51, 259–263.

Götze, W. (1991) Aspects of structural glass transitions. In J.P. Hansen, D. Levesque, and J. Zin-Justin, Eds., Liquids, freezing, and glass transition, Volume 1, p. 292–503. Elsevier, Amsterdam.

Hess, K-U. (1996) Zur Temperaturabhängigkeit der Viscosität von haplogranitischen Schmelzen. Ph.D. thesis, Universität Bayreuth, Germany.

Hess, K-U., Dingwell, D.B., and Webb, S.L. (1995) The influence of excess alkalis on the viscosity of a haplogranitic melt. American Mineralogist, 80, 297–304.

Hummel, W. and Arndt, J. (1985) Variation of viscosity with temperature and composition in the plagioclase system. Contributions to Mineralogy and Petrology, 90, 83–92.

Hunold, V.K. and Brückner, R. (1980) Physikalische Eigenschaften und struktereller Feinbau von Natrium-Aluminosilicatgläsern und-schmelzen. Glastechische Berichte, 6, 149–161.

Lacy, E.D. (1963) Aluminum in glasses and melts. Physics and Chemistry of Glasses, 4, 234–238.

Loewenstein, W. (1954) The distribution of aluminium in the tetrahedra of silicates and aluminates. American Mineralogist, 39, 92–96.

Maekawa, H., Maekawa, T., Kawamura, K., and Yokokawa, T. (1991) ^{29}Si MAS NMR investigation of the Na_2O-Al_2O_3-SiO_2 glasses. Journal of Physical Chemistry, 95, 6822–6827.

Matson, D.W., Sharma, S.K., and Philpotts, J.A. (1986) Raman spectra of some tectosilicates and glasses along the orthoclase-anorthite and nepheline-anorthite joins. American Mineralogist, 71, 694–704.

Mazurin, O.V., Streltsina, M.V., and Shvaiko-shvaikovskaya, T.P. (1987) Handbook of glass data. Part C: Ternary silicate glasses. Physical Sciences Data 15, p. 1110. Elsevier, Amsterdam.

——— (1993) Handbook of glass data. Part E: Supplement to parts A-D. Physical Sciences Data 15, p. 875, Elsevier.

McMillan, P., Piriou, B., and Navrotsky, A. (1982) A Raman spectroscopic

study of glasses along the joins silica-calcium aluminate, silica-sodium aluminate, and silica-potassium aluminate. Geochimica et Cosmochimica Acta, 46, 2021–2037.

Murdoch, J.B., Stebbins, J.F., and Carmichael, I.S.E. (1985) High-resolution ^{29}Si NMR study of silicate and aluminosilicate glasses: the effect of network modifying cations. American Mineralogist, 70, 332–343.

N'Dala, I., Cambier, F., Anseau, M.R., and Urbain, G. (1984) Viscosity of liquid feldspars Part 1: Viscosity measurements. British Ceramic Transactions and Journal, 83, 105–107.

Navrotsky, A., Peraudeau, G., McMillan, P., and Coutures, J-P. (1982) A thermochemical study of glasses and crystals along the joins silica-calcium aluminate and silica-sodium aluminate. Geochimica et Cosmochimica Acta, 46, 2039–2047.

Neuville, D.R. (1992) Etude des propriétés thermodynamiques et rhéologiques des silicates fondus. Ph.D. thesis, Université de Paris 7—spécialité géochimie fondamentale.

Neuville, D.R. and Mysen, B.O. (1996) Role of aluminium in the silicate network: In situ high-temperature study of glasses and melts on the join SiO_2-$NaAlO_2$. Geochimica et Cosmochimica Acta, 60, 1727–1737.

Neuville, D.R. and Richet, P. (1991) Viscosity and mixing in molten (Ca, Mg) pyroxenes and garnets. Geochimica et Cosmochimica Acta, 55, 1011–1019.

Oestrike, R., Yang, W.H., Kirkpatrick, J., Hervig, R.L., Navrotsky, A., and Montez, B. (1987) High-resolution ^{23}Na, ^{27}Al and ^{29}Si NMR spectroscopy of framework-aluminosilicate glasses. Geochimica et Cosmochimica Acta, 51, 2199–2210.

Plazek, D.J. and Ngai, K.L. (1991) Correlation of polymer segmental chain dynamics with temperature dependent time-scale shifts. Macromolecules, 24, 1222–1224.

Richet, P. (1984) Viscosity and configurational entropy of silicate melts. Geochimica et Cosmochimica Acta, 48, 471–483.

Richet, P. and Bottinga, Y. (1984) Glass transitions and thermodynamic properties of amorphous SiO_2, $NaAlSi_nO_{2n+2}$ and $KAlSi_3O_8$. Geochimica et Cosmochimica Acta, 48, 453–470.

——— (1985) Heat capacity of aluminum-free liquid silicates. Geochimica et Cosmochimica Acta, 49, 471–486.

——— (1995): Rheology and configurational entropy of silicate melts. In Mineralogical Society of America Reviews in Mineralogy 32, 67–93.

Richet, P. and Neuville, D.R. (1992) Thermodynamics of silicate melts: configurational properties. In S. Saxena, Ed., Thermodynamic Data. Systematics and Estimation, Advances in Physical Geochemistry, p. 132–160. Springer-Verlag, Berlin.

Richet, P., Robie, R.A., Rogez, J., Hemingway, B.S., Courtial, P., and Tequi, C. (1990) Thermodynamics of open networks: Ordering and entropy in $NaAlSiO_4$ glass, liquid, and polymorphs. Physics and Chemistry of Minerals, 17, 385–394.

Riebling, E.F. (1966) Structure of sodium aluminosilicate melts containing at least 50 mole% SiO_2 at 1500°C. Journal of Chemical Physics, 44, 2857–2865.

Scamehorn, C. and Angell, C.A. (1991) Viscosity-temperature relations and structure in fully polymerised aluminosilicate melts from ion dynamics simulations. Geochimica et Cosmochimica Acta, 55, 721–730.

Shaw, H.R. (1972) Viscosities of magmatic silicate liquids: an empirical method of prediction. American Journal of Science, 272, 870–893.

Seifert, F.A., Mysen, B.O., and Virgo, D. (1982) Three-dimensional network structure of quenched melts (glass) in the systems SiO_2-$NaAlO_2$, SiO_2-$CaAl_2O_4$ and SiO_2-$MgAl_2O_4$. American Mineralogist, 67, 696–717.

Stein, D.J. and Spera, F.J. (1993) Experimental rheometry of melts and supercooled liquids in the system $NaAlSiO_4$-SiO_2: Implications for structure and dynamics. American Mineralogist, 78, 710–728.

——— (1995) Molecular dynamics simulations of liquids and glasses in the system $NaAlSiO_4$-SiO_2: Methodology and melt structures. American Mineralogist, 80, 417–431.

Tauber, P. and Arndt, J. (1987) The relationship between viscosity and temperature in the system anorthite-diopside. Chemical Geology, 62, 71–81.

Taylor, M. and Brown, G.E. (1979) Structure of mineral glasses'II. The SiO_2-$NaAlSiO_4$ join. Geochimica et Cosmochimica Acta, 43, 1467–1475.

Taylor, T.D. and Rindone, G.E. (1970) Properties of aluminosilicate glasses. V. Low temperature viscosities. Journal of the American Ceramic Society, 53, 692–695.

Toplis, M.J. and Dingwell, D.B. (1996) The variable influence of P_2O_5 on the viscosity of melts of differing alkali/aluminium ratio: Implications for the structural role of phosphorus in silicate melts. Geochimica et Cosmochimica Acta, 60, 4107–4121.

Toplis, M.J., Dingwell, D.B., and Lenci, T. (1997) Peraluminous viscosity maxima in Na_2O-Al_2O_3-SiO_2 liquids: The role of triclusters in tectosilicate melts. Geochimica et Cosmochimica Acta, 61, 2605–2612.

Manuscript received September 30, 1996
Manuscript accepted May 12, 1997